LA-UR-21-26581
Approved for public release; distribution is unlimited.

Title: Estimates of Acoustic to Seismic Coupling Over Topography from Time Domain Numerical Modeling

Author(s): Bishop, Jordan Wilson
Fee, David
Modrak, Ryan Thomas
Tape, Carl
Kim, Keehoon

Intended for: Coffee & Geophysics Talk via WebEx

Issued: 2021-07-12

Estimates of Acoustic to Seismic Coupling Over Topography from Time Domain Numerical Modeling

Jordan W. Bishop*, David Fee, Ryan Modrak, Carl Tape, and Keehoon Kim

Coffee & Geophysics Seminar
07/15/2021

Motivation

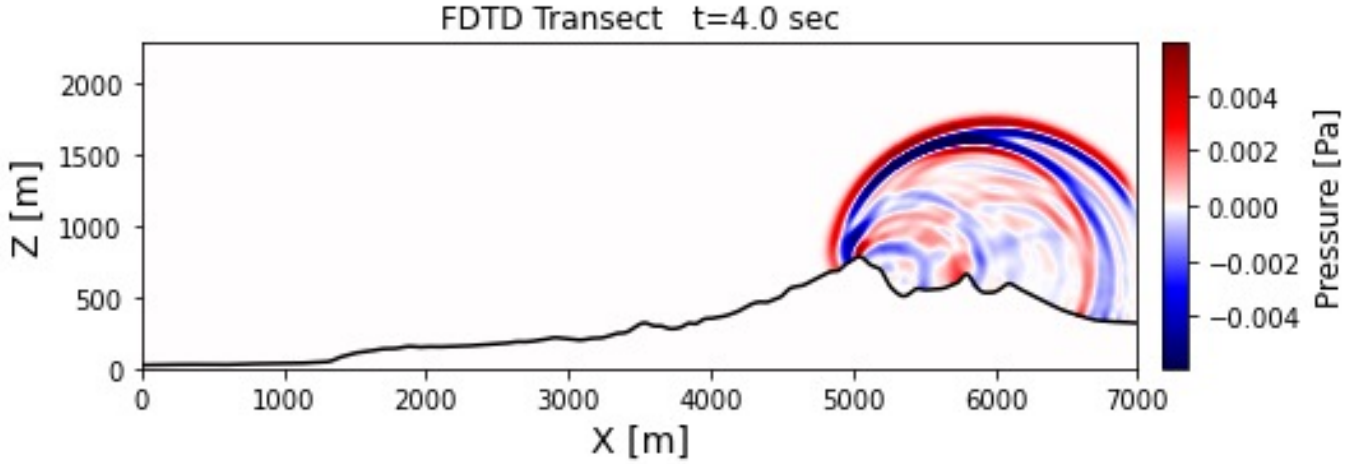

infraFDTD3D – Finite Difference Time Domain infrasound propagation code (Kim and Lees, 2011).

1. A *rigid boundary condition* is typically applied in infrasound propagation, which prohibits refraction and ground loading from incident acoustic waves.
2. However, acoustic-to-seismic coupled waves are somewhat commonly observed, and they have been observed up to approximately 500 km away.
3. Near surface seismic speeds (such as a generic volcano velocity model) can potentially less than the atmospheric adiabatic sound speed (e.g. Lesage et al. 2018).

How can we quantify the effect of acoustic to seismic coupling on infrasound observations?

Content

1. Introduction to terms and definitions
2. Build understanding with propagation over elastic halfspaces
3. Propagation over topography

Acoustic and Seismic Solver: SPECFEM3D

- We simulate both acoustic and seismic waves with the spectral element code SPECFEM3D (Komatitsch and Tromp, 1999).

- SPECFEM3D accommodates full acoustic-to-seismic coupling.
  1. Displacement is continuous normal to the interface (the ground surface).
  2. Traction normal to the interface is continuous across the boundary.

     (free slip boundary condition)

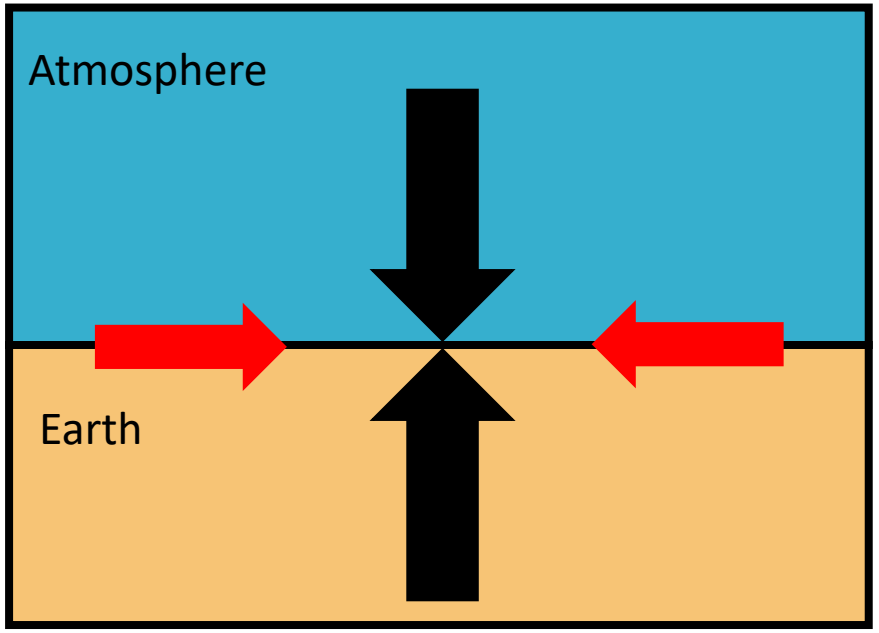

Coupling Quantification: Energy Admittance

- The ratio of seismic kinetic energy density to acoustic kinetic energy density (Albert and Orcutt, 1989; Edwards et al. 2007).

$$EA = \frac{(1/2)\rho_s v^2_{\text{seismic}}}{(1/2)\rho_f v^2_{\text{acoustic}}}$$

- Particle velocity values for both acoustic and seismic receivers are directly obtained from the simulations (no impedance-based conversion from pressure).

Analytical Model: Spherical Coupling Coefficients

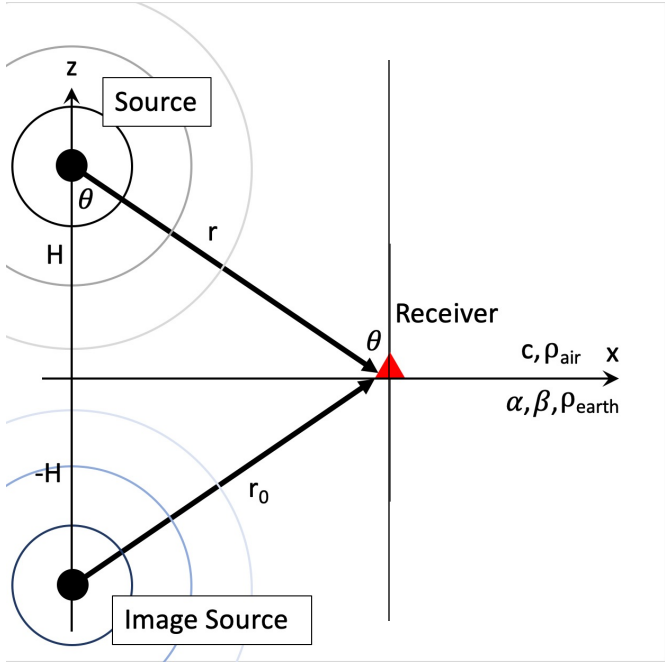

Schematic depicting a spherical acoustic wave impinging on an elastic halfspace. Note that θ is the angle from the vertical axis.

Spherical wave acoustic coupling coefficients are decidedly more complex than planar reflection and transmission coefficients (e.g. Roever et al. 1959).

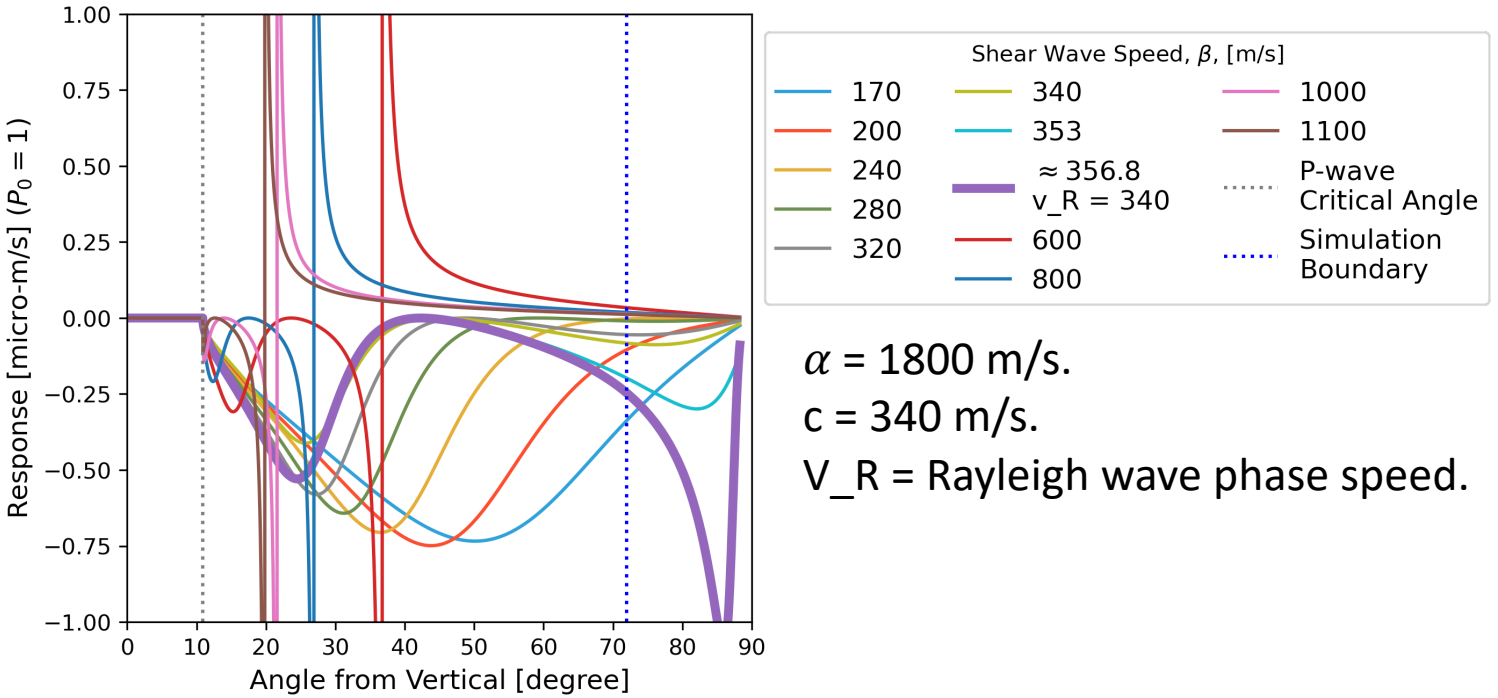

α = 1800 m/s.
c = 340 m/s.
V_R = Rayleigh wave phase speed.

Halfspace Propagation

- Isotropic moment tensor source placed 1500 m above the planar surface separating acoustic and elastic media.
- Receivers placed on both sides of the boundary between the two media.

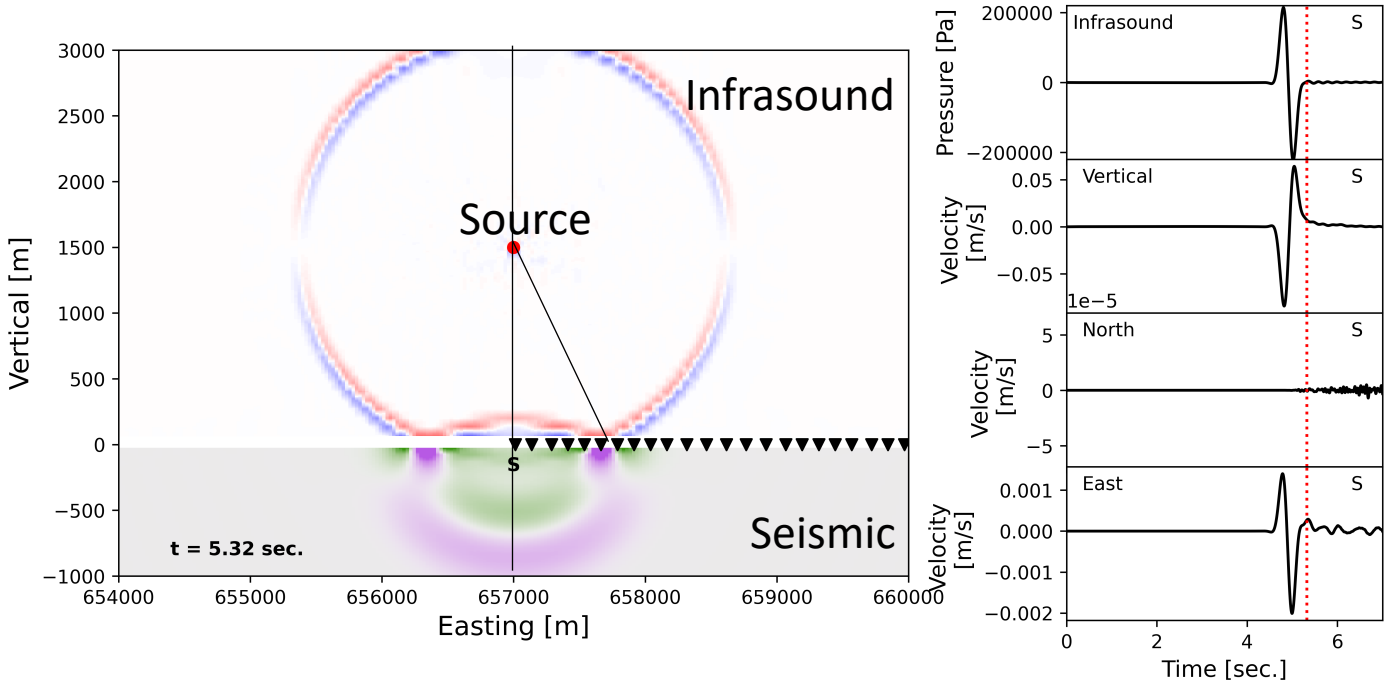

Left: Cross section of simulation domain showing the vertical particle motion in both the acoustic and seismic domains. Right: Simulated waveforms at receiver ‘S’. The pressure in the acoustic medium is on the top plot, and the three components of the seismic receiver (Z, N, E) are below it.

Halfspace Propagation

- Varying the P-wave speed (α), but keeping the shear wave speed (β) constant.

- After the peak values at vertical incidence (11.2%), secondary energy admittance peaks form at shallower angles of incidence.

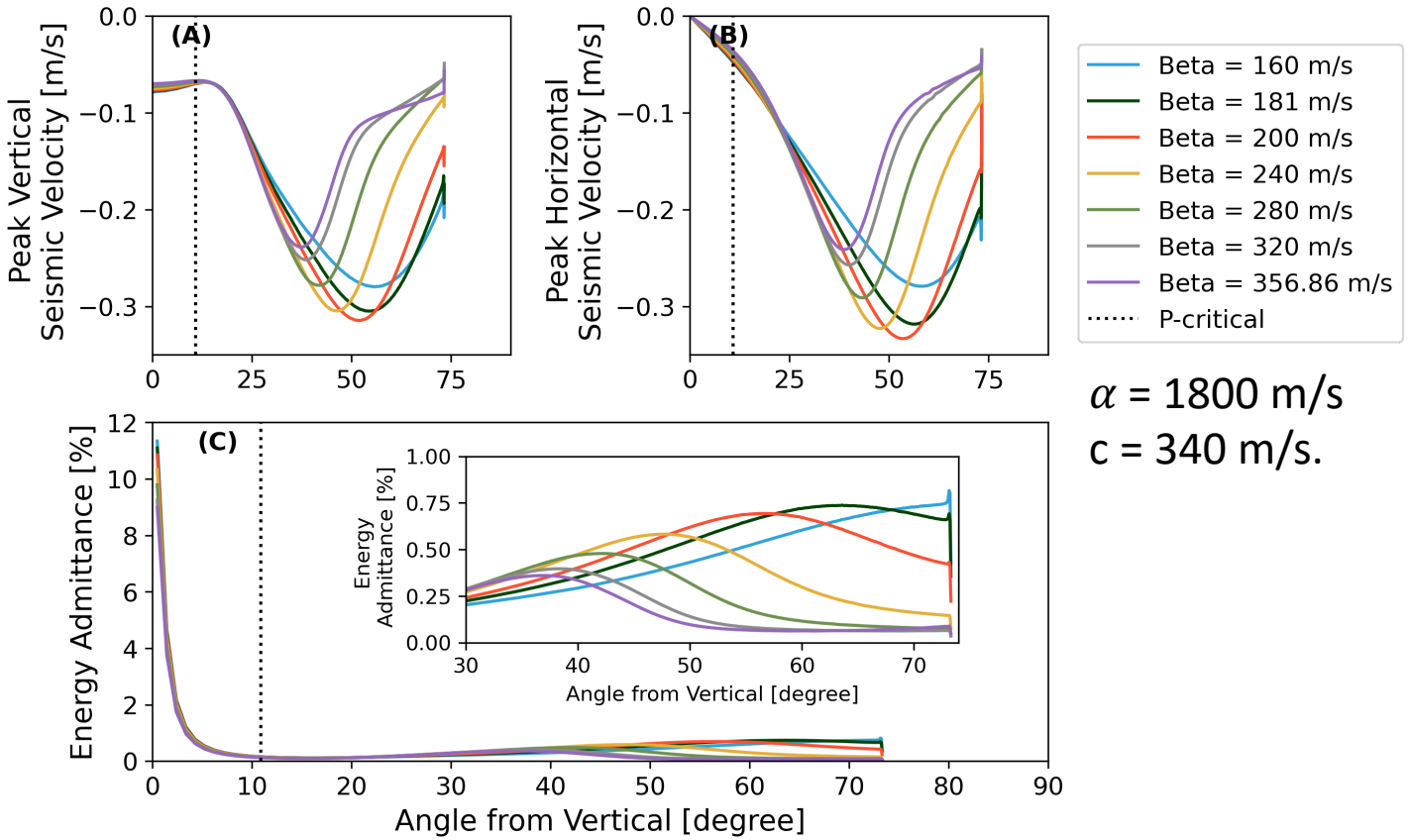

α = 1800 m/s
c = 340 m/s.

- Energy admittance peaks decrease with increasing shear wave speed.

Halfspace Propagation

- Varying the P-wave speed (α), but keeping the shear wave speed (β) constant.

- The largest energy admittances again occur at near vertical incidence (~30 %), and secondary energy admittance peaks again form.

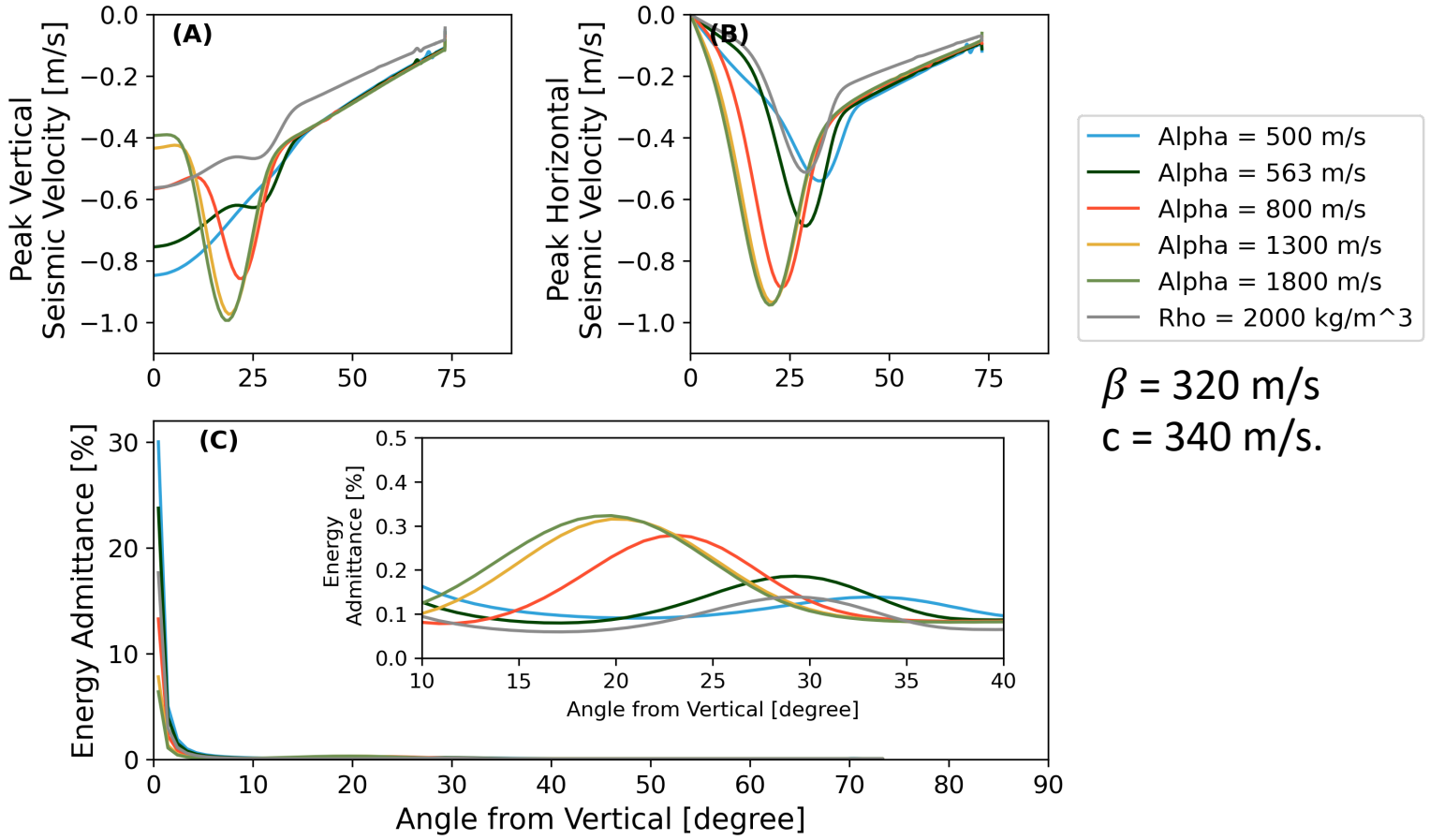

β = 320 m/s
c = 340 m/s.

- Energy admittance peaks decrease with increasing P-wave speed.

Halfspace Propagation – 3 Specific Models

1. Case 4 - A ”reflective model” - approximates a rigid boundary in our simulations.
α = 3000 m/s, β = 2000 m/s ,
ρ = 2000 kg/m^3.

2. Case 5 - A model approximating the top layer of the generic volcano velocity model (Lesage et al. 2018).
α = 540 m/s, β = 320 m/s ,
ρ = 1492 kg/m^3.

3. Case 6 - A model approximating the top layer of the Edwards et al. 2007 velocity model.
α = 1344 m/s, β = 178 m/s ,
ρ = 2020 kg/m^3.

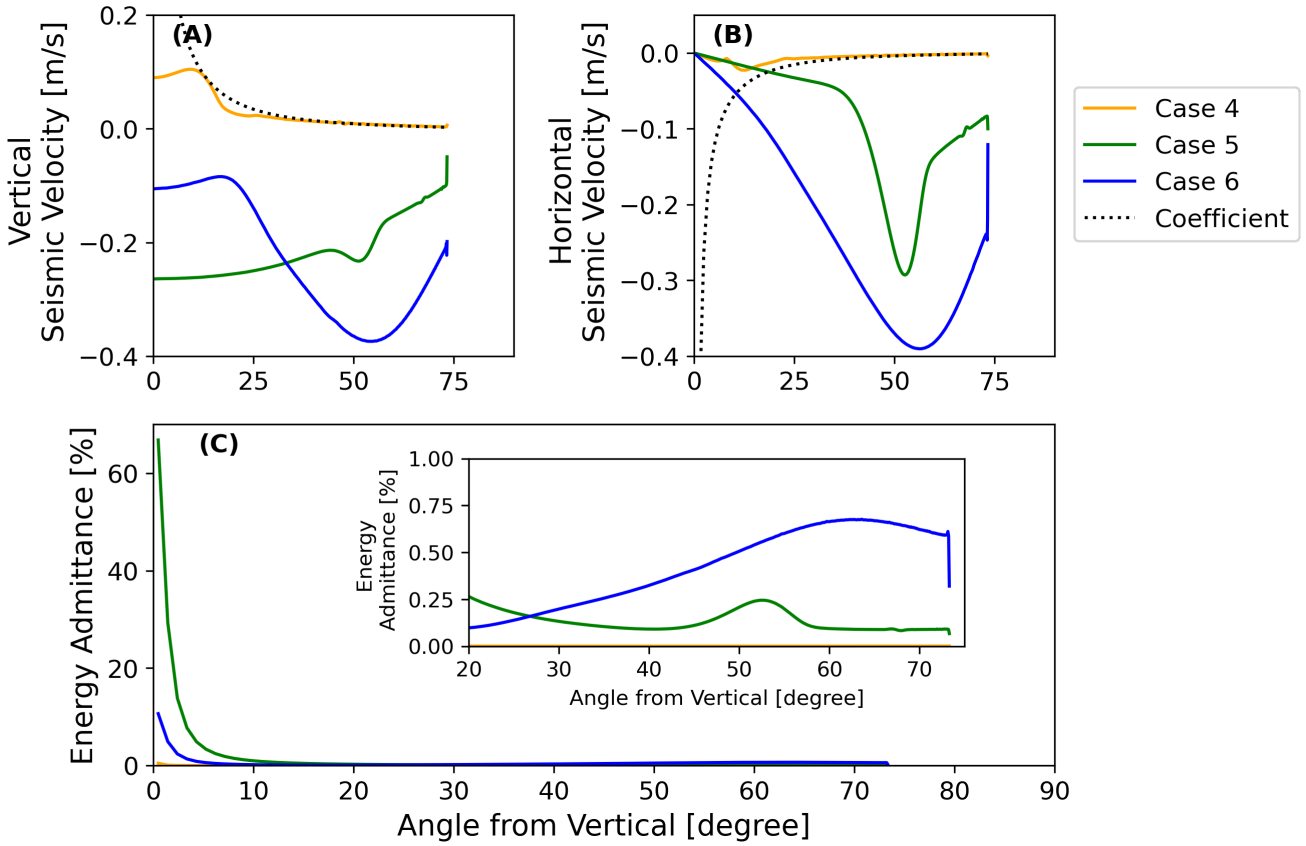

- The energy admittance for the reflective model (Case 4) is << 1% for all angles of incidence. Case 5 has the largest energy admittance value in this study (67%).

Propagation over Topography – Sakurajima Volcano, Japan

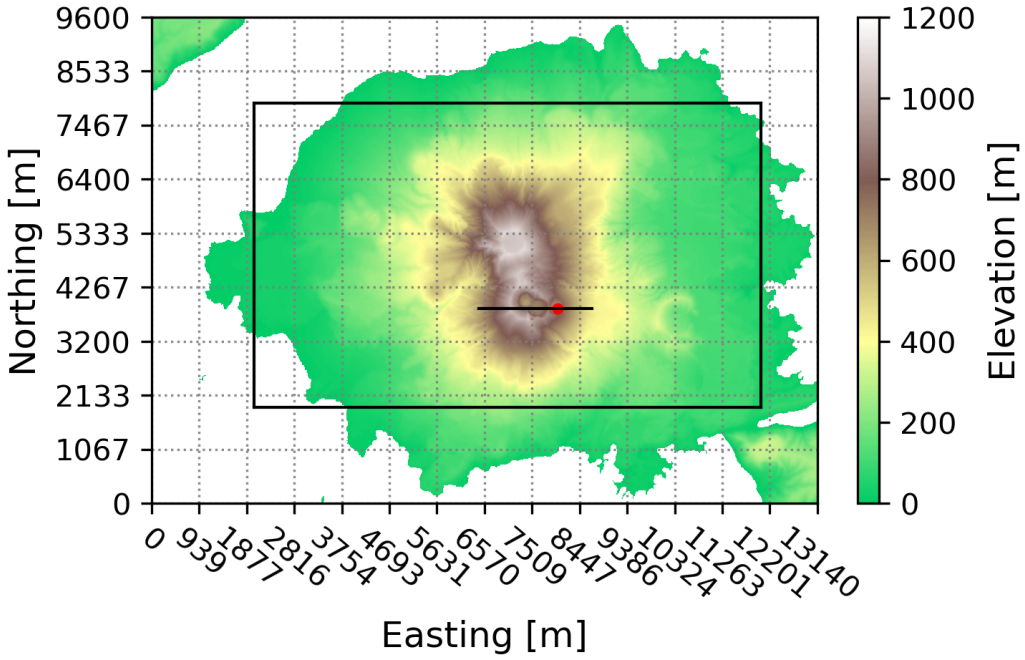

Map view of Sakurajima Volcano, Japan. The simulation domain is bounded by the black box, and the source location is denoted by the red point.

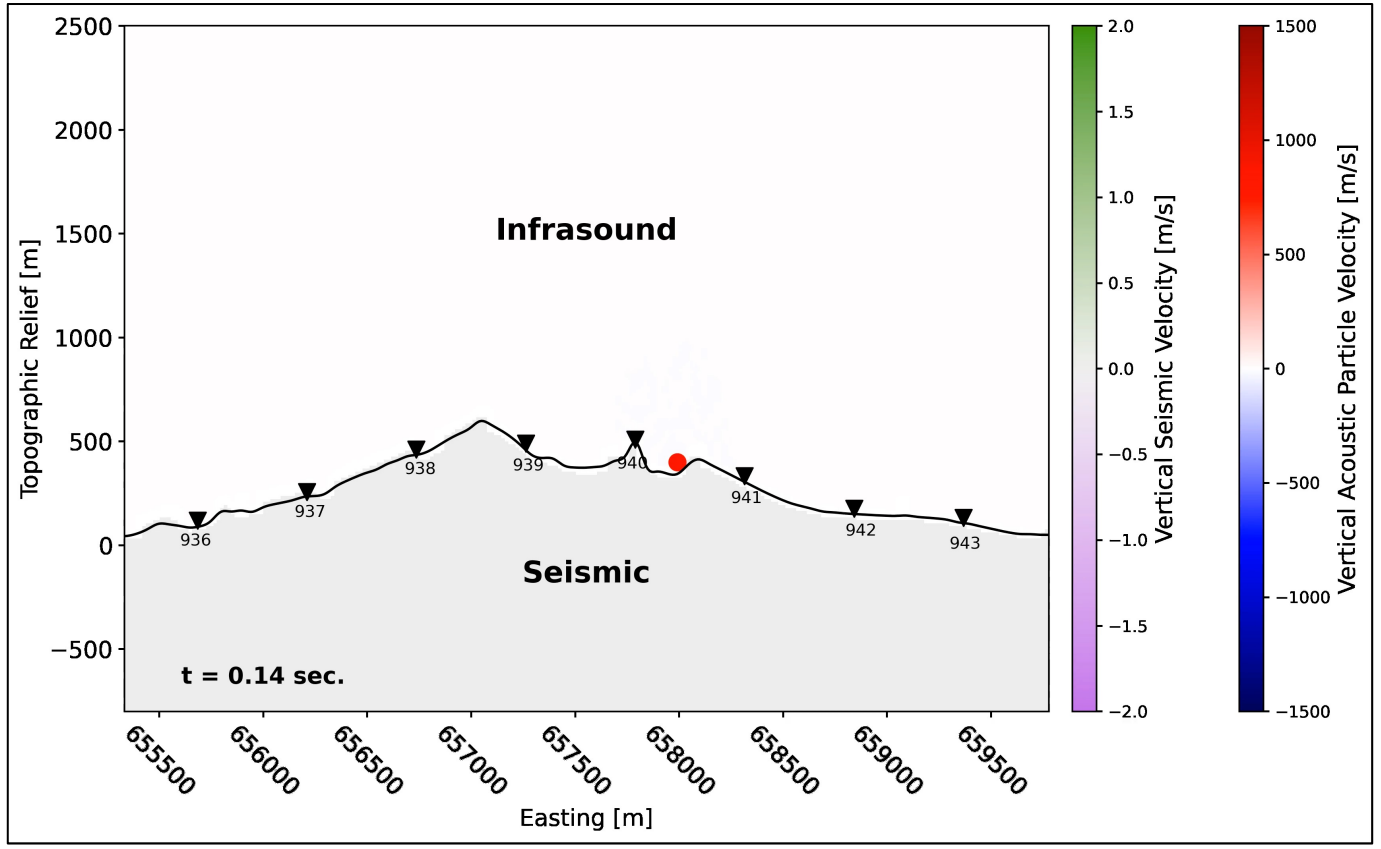

Vertical component of the acoustic and seismic particle velocities in the cross section denoted in the map view plot.

Propagation over Topography

Same source and receiver configuration as halfspace simulations.

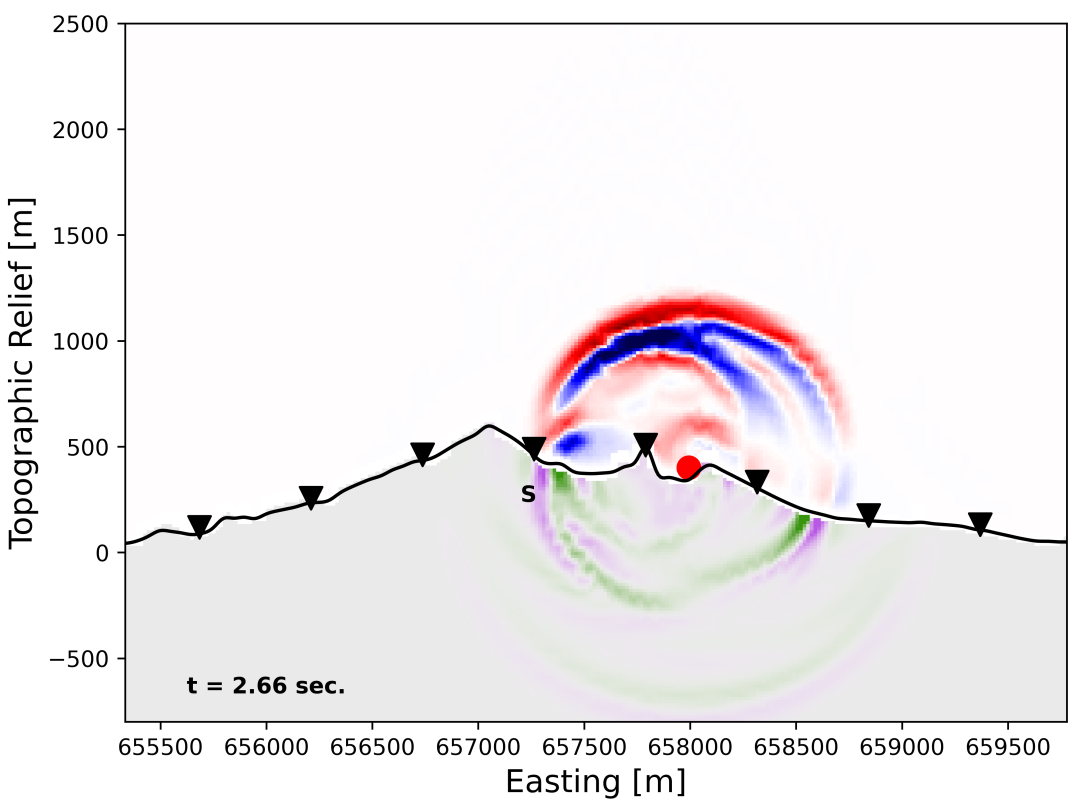

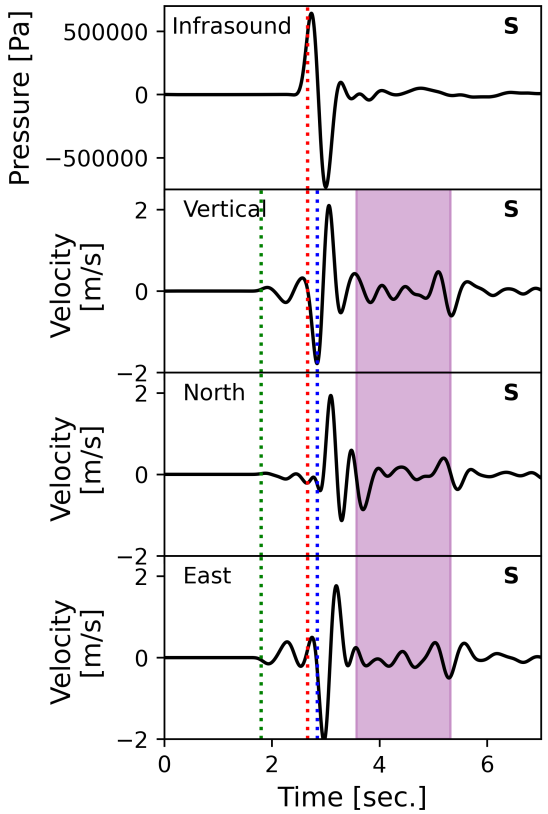

Green: P-wave arrival
Red: Time in simulation plot
Blue: Acoustic wave arrival
Purple: Rayleigh wave arrival

Left: Cross section of simulation domain showing the vertical particle motion in both the acoustic and seismic domains.
Right: Simulated waveforms at receiver ‘S’. The pressure in the acoustic medium is on the top plot, and the three components of the seismic receiver (Z, N, E) are below it.

Propagation over Topography – Energy Admittance

- To estimate an upper bound on the energy admittance, we try an notably slow elastic model (Case 7):
  α = 300 m/s, β = 200 m/s ,
  ρ = 1492 kg/m^3.

- The peak value of the energy admittance is approximately 7.8%, and the largest admittance occurs to the west and south of the source (red).

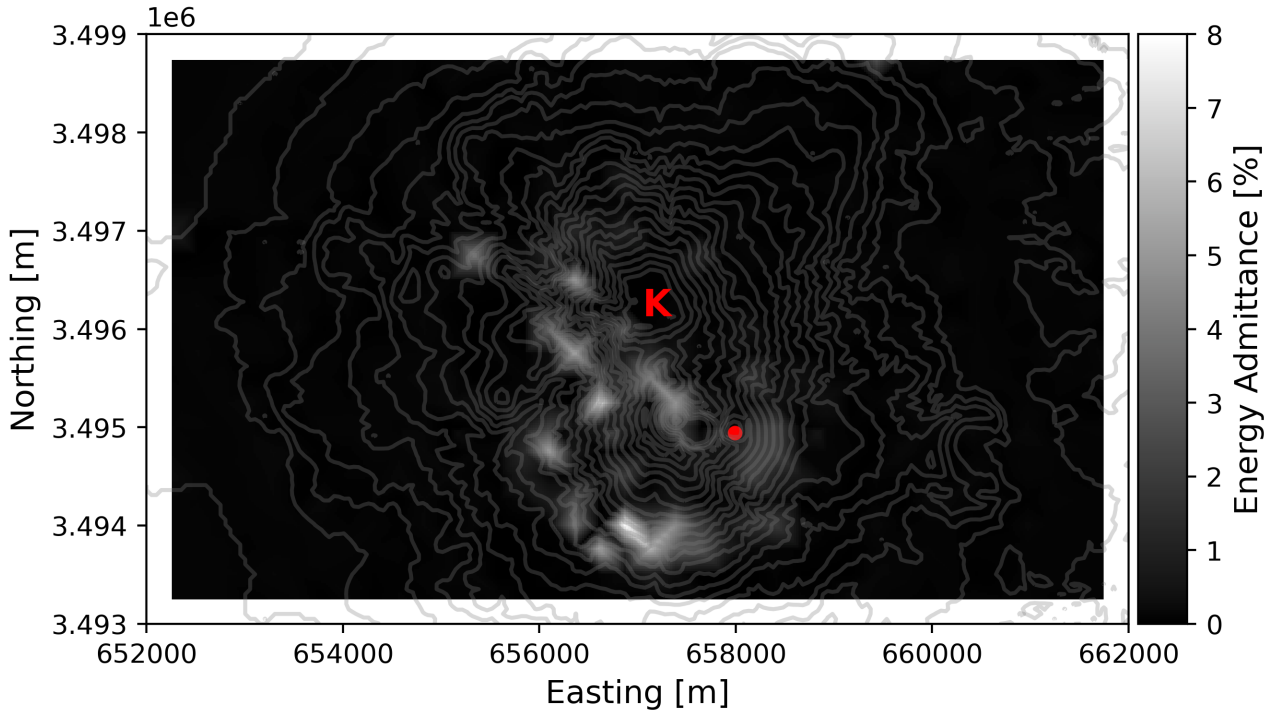

Propagation over Topography – Energy Admittance

We interpret the overall pattern in energy admittance to be the result of a complex distribution of incidence angles.

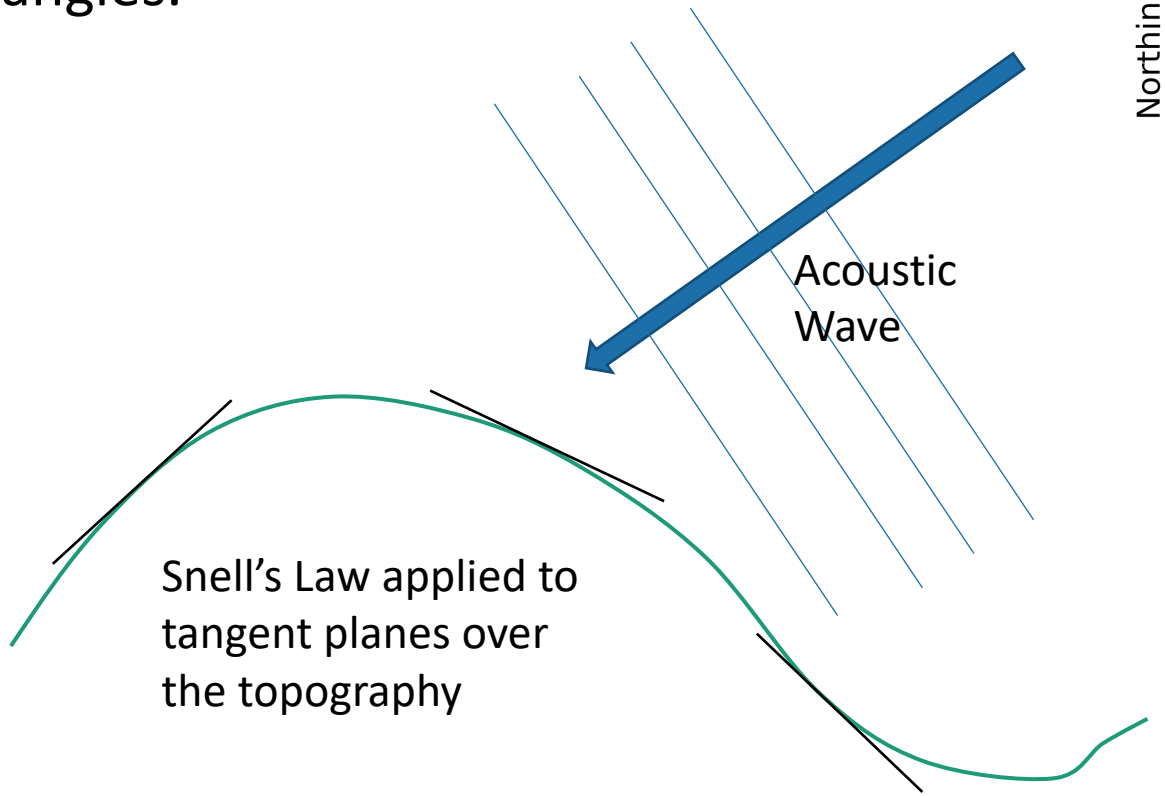

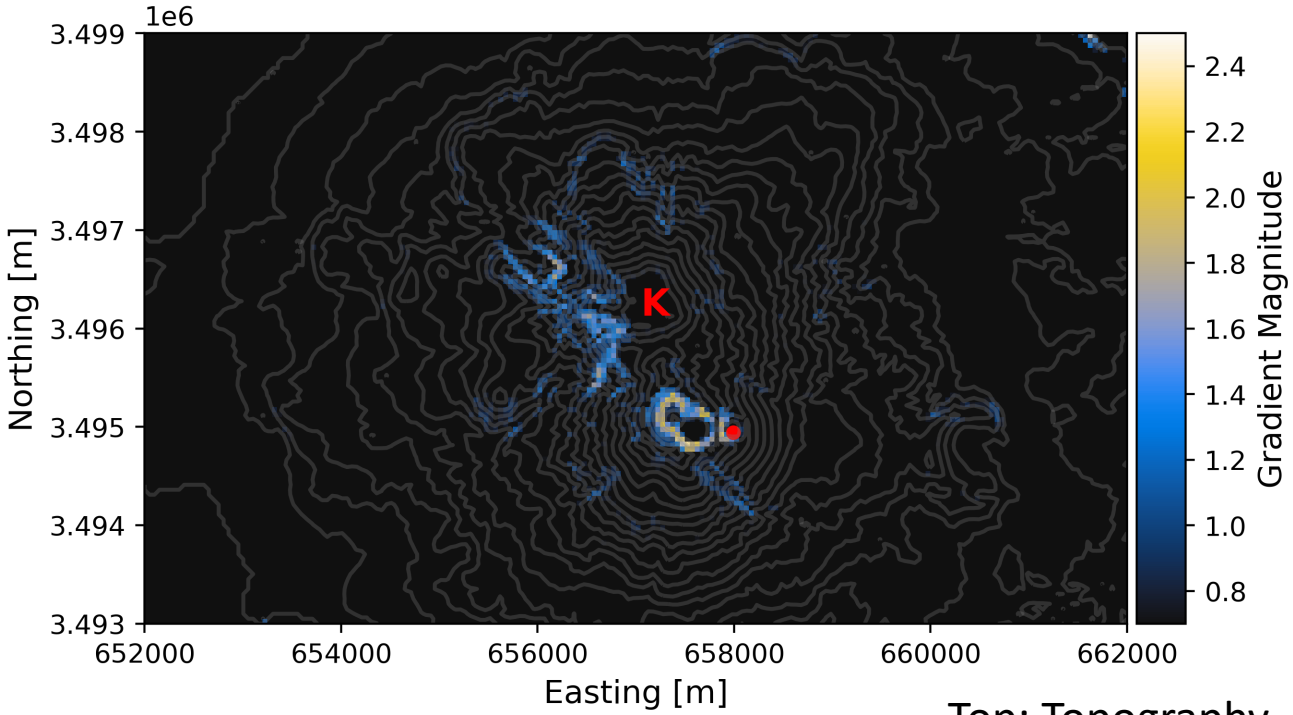

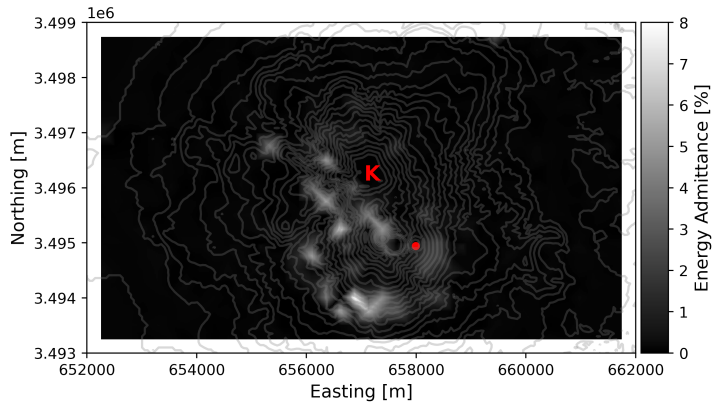

Top: Topography Gradient Magnitude

Propagation over Topography

- Interference in the time domain between the seismic surface wave and the ground coupled airwave can bias energy admittance estimates.
- (A): We examine the relative difference in peak pressure between the Lesage et al. (2018) type model (Case 5) and the “reflective” model (Case 4).
- (B): We examine the relative difference in peak pressure between our soft model (Case 7) and the “reflective” model (Case 4).
- These plots show the relative difference in observed peak pressure as a result of acoustic to seismic coupling over the propagation path for each model.

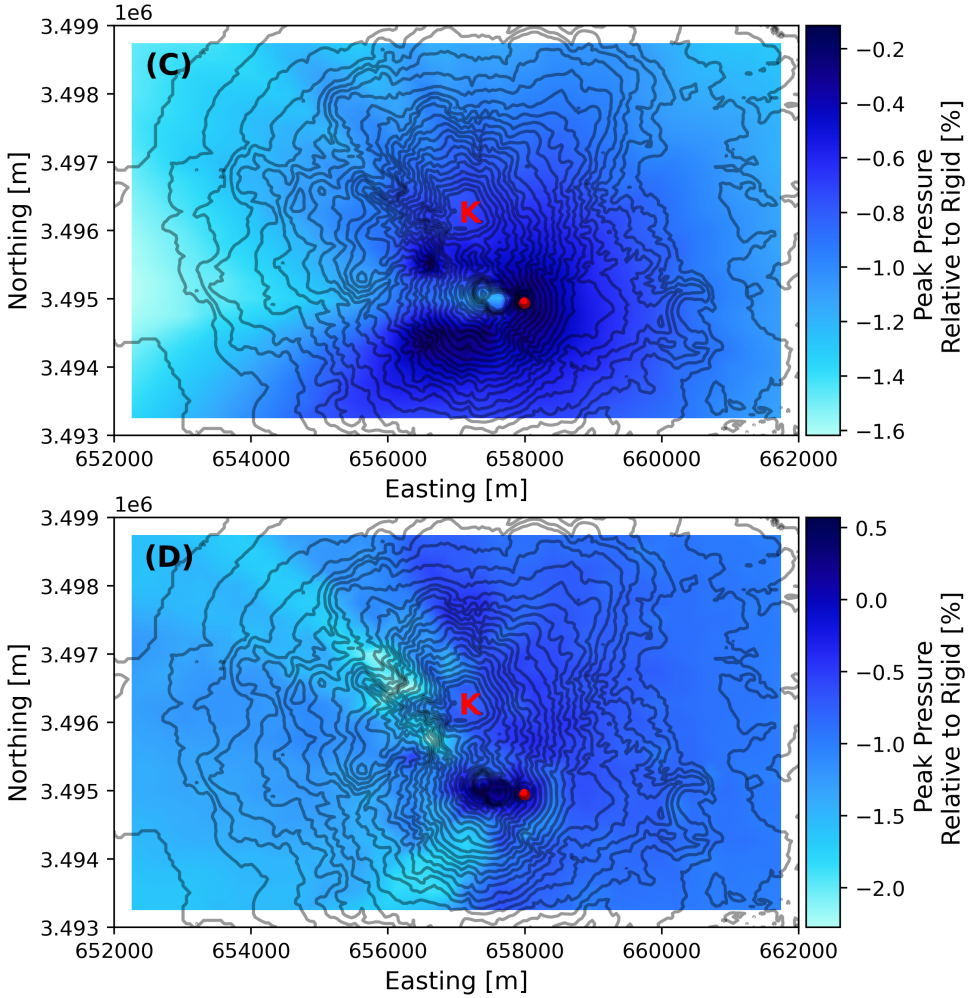

Future Work

- Uncertainty quantification for coupling values.
- Homogeneous elastic halfspaces are used here, but a layered elastic halfspace would admit dispersion into the coupling. A frequency domain method (with topography) would better determine how infrasound waves interact with layered earth.
- Wind is important for infrasound propagation, and it is not included in SPECFEM3D. In the near field, moving media may introduce some slight directionality to acoustic to seismic coupling patterns.
- The cumulated effect of acoustic to seismic coupling over long ranges (multiple acoustic “bounce points”) is still unquantified.

Conclusions

- For halfspace models shown here, we see energy admittance values up to ~67% over a limited spatial area.

- When considering topography, complex spatial trends appear in the energy admittance calculations. We connect this pattern to the incidence angles of the propagating infrasound wave and note a relative pressure difference of up to 2% on the models considered here.

Spherical Coupling Equations (Roever et al. 1959)

$$A(u) = \frac{\gamma R(u) - (\rho_f/\rho_s)K_2^4\chi}{\gamma R(u) + (\rho_f/\rho_s)K_2^4\chi},$$

Reflection Coefficient

For $t_p \le t \le \frac{r}{c}$ or $K_1 \le u \le \frac{x}{r}$:

$$p_1^f(x,z;\mathrm{delta}) = \frac{2(\rho_f/\rho_s)cK_2^4P_0}{r\delta}\left[\frac{\gamma(K_2^2-2u^2)^2\sqrt{u^2-K_1^2}}{\gamma^2(K_2^2-2u^2)^4 - \chi_t^2\{4u^2\psi_t\gamma + (\rho_f/\rho_s)K_2^4\}^2}\right];$$

$$\dot{U}(x,z=H;\mathrm{delta}) = \frac{u\left[2\psi\gamma + (\rho_f/\rho_s)K_2^2\right])}{K_2^2-2u^2} \cdot \frac{p^f(\mathrm{delta})}{\rho_f c};$$

$$\dot{W}(x,z=H;\mathrm{delta}) = -\gamma \cdot \frac{p^f(\mathrm{delta})}{\rho_f c};$$

Response Functions

(19)

Acoustic-Seismic Source Scaling

- SPECFEM3D requires a moment tensor source.
- To relate our simulations to the infrasound literature, we want to construct an equivalent acoustic monopole from an isotropic moment tensor with seismic moment M_0.
- Previously examined by Longonne (1994, 2016), Aldridge (2000), Haney (2018), and others.

- Two approaches:
  1. Derive acoustic quadrupole components from the moment tensor-equivalent body force.
  2. Show equivalence between a moment tensor and acoustic quadrupole by equating their volumetric definitions, i.e. “stress glut” in seismology and Lighthill’s acoustic analogy in acoustics.

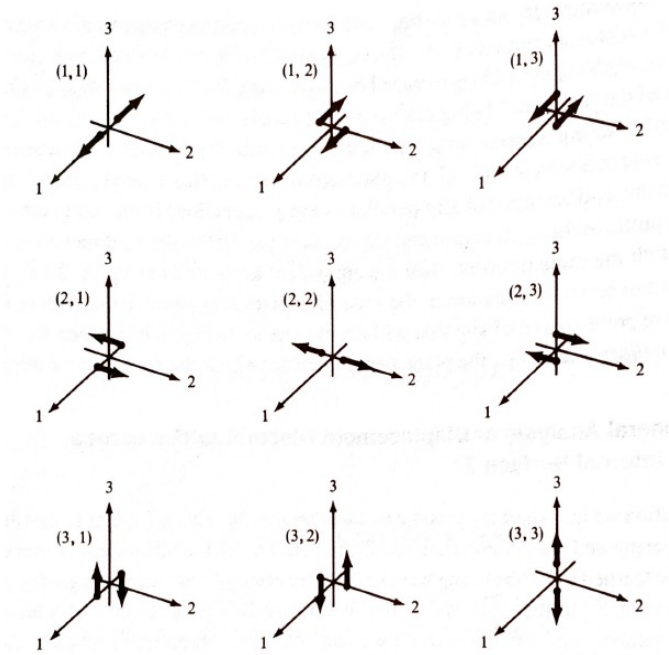

Moment Tensor Double Couple Forces
Aki and Richards, 2004

1. Equivalent Body Force Approach

$$\frac{1}{c^2}\frac{\partial^2 p}{\partial t^2} - \nabla^2 p = -(\nabla \cdot \mathbf{F}(t)).$$

Start: Inhomogeneous Wave Equation

$$\mathbf{F} = -\mathbf{M} \cdot \nabla \delta(\mathbf{x} - \mathbf{x}_{\text{src}}) K(t),$$

Substitute Equivalent Body Force

$$\frac{1}{c^2}\frac{\partial^2 p}{\partial t^2} - \nabla^2 p = K(t) \sum_i M_{ii} \frac{\partial^2}{\partial x_i^2} \delta(\mathbf{x} - \mathbf{x}_{\text{src}}).$$

Inhomogeneous Wave Equation

Solve with Green's Function

$$\hat{p}(\omega) = \sum_{j=1}^{3} \hat{Q}_{jj} \frac{\partial^2}{\partial x_j^2} \frac{e^{ikr}}{r} = \sum_{j=1}^{3} \left(M_{jj} \hat{K}(\omega) \right) \frac{\partial^2}{\partial x_j^2} \frac{e^{ikr}}{4\pi r}$$

Frequency domain quadrupole representation (e.g. Pierce, 1989)

After grouping terms, we recognize that this is the pressure field from an acoustic quadrupole source.

Previously shown by Haney et al. 2018

2. Generalized Stress Glut Approach

- A seismic moment tensor is the volume integral of stress glut rate over the source region (e.g. Dahlen & Tromp, 1998).

$$\mathbf{M} = \int_{t_0}^{t_f} \int_{V_{\mathrm{src}}} \partial_t \mathbf{S} dV$$

- An acoustic quadrupole (tensor) is also defined as the volumetric integral of a stress term over the source region.

$$T_{ij} = (B_{ij} + \rho v_i v_j) - p\delta_{ij}$$

Turbulent Acoustic Source (Lighthill, 1952)

$$Q(t) = \int_{t_0}^{t_f} \int_{V_{\mathrm{src}}} T dV$$

$$\mathbf{\Pi} = (p_{\mathrm{true}} - p_{\mathrm{Hooke}})\mathbf{I} + \rho\vec{v}\vec{v}.$$

"Stress-Momentum Glut" (Lognonne et al., 1994; 2016)

Special Case: An isotropic moment tensor

- In the case that the moment tensor is isotropic, we get this equation in the time domain:
- The pressure is omnidirectional, so it is a monopole source field.
- Pressure from a conventional monopole acoustic source (mass source) is typically written

$$p(\mathbf{x},t) = \frac{M_0}{4\pi R c^2}\ddot{K}\left(t-\frac{R}{c}\right).$$

R – Distance
c – Acoustic wave speed
M_0 - Seismic moment
K – Seismic source time function

$$\frac{M_0}{c^2}\ddot{K}\left(t-\frac{R}{c}\right) = \dot{S}\left(t-\frac{R}{c}\right).$$

How moment acceleration scales to mass flow acceleration.
Previously suggested in a different form by Aldridge, 2000

$$p(\mathbf{x},t) = \frac{1}{4\pi R}\dot{S}\left(t-\frac{R}{c}\right),$$

R – Distance
S – Mass flow rate per unit time (acceleration)